

1 Article

2 Zebrafish Otolith Biomineralization Requires 3 Polyketide Synthase

4 Kevin D. Thiessen¹, Lisa Higuchi¹ and Kenneth L. Kramer^{1,*}

5 ¹ Department of Biomedical Sciences, Creighton University School of Medicine, Omaha, NE, United States

6 * Correspondence: kenkramer@creighton.edu; Tel.: +1 402-280-2763

7 **Abstract:** Deflecting biomineralized crystals attached to vestibular hair cells is necessary for
8 maintaining balance. Zebrafish (*Danio rerio*) are useful organisms to study these biomineralized
9 crystals called otoliths as many required genes are homologous to human otoconial development.
10 We sought to identify and characterize the causative gene in a pair of genetically-linked mutants, *no*
11 *content* (*nco*) and *corkscrew* (*csr*), that fail to develop otoliths during early ear development. We show
12 that *nco* and *csr* have potentially deleterious mutations in polyketide synthase (*pks1*), a multi-modular
13 protein that has been previously implicated in biomineralization events in chordates and
14 echinoderms. We found that Otoconin-90 (Oc90) expression within the otocyst is normal in *nco* and
15 *csr*; therefore, it is not sufficient for otolith biomineralization in zebrafish. Similarly, normal
16 localization of Otogelin, a protein required for otolith tethering in the otolithic membrane, is not
17 sufficient for Oc90 attachment. Furthermore, eNOS signaling and Endothelin-1 signaling were the
18 most up- and down-regulated pathways during otolith agenesis in *nco*, respectively. Our results
19 demonstrate distinct processes for otolith nucleation and biomineralization in vertebrates and will be
20 a starting point for models that are independent of Oc90-mediated seeding. Furthermore, this study
21 will serve as a basis for investigating the role of eNOS signaling and Endothelin-1 signaling during
22 otolith formation.

23 **Keywords:** inner ear, otolith, biomineralization, calcium carbonate, polyketide synthase, zebrafish,
24 endothelin-1, eNOS

25

26 1. Introduction

27 Oтоconia and otoliths act as a mass load that increase the sensitivity of mechanosensory hair
28 cells to the effects of gravity and linear acceleration in mammals and fish, respectively. While the
29 morphology of otoconia (“ear particles”) and otoliths (“ear stones”) differ, the initial formation of
30 bio-crystals rely on many homologous proteins [1]. Zebrafish otoliths are primarily composed of
31 calcium carbonate in the form of aragonite, which accounts for ~99% of the total otolithic mass [2, 3].
32 The center of the otolith contains a proteinaceous core that acts as a site for otolith nucleation and
33 biomineralization. This matrix lays the foundation for further otolith growth, which is mediated by
34 daily deposition of additional otoconins and calcium carbonate molecules [2].

35 In zebrafish, otolith nucleation occurs when the otolith precursor particles or OPPs bind to the
36 tips of the immotile kinocilia of tether cells within the otic vesicle [4, 5]. Subsequent studies have
37 demonstrated that the critical period of otolith seeding and nucleation starts at 18-18.5 hpf and ceases
38 by 24 hpf. [1, 4, 6-8]. In mammalian inner ear development, Otoconin-90 (Oc90; the major protein
39 component of otoconia) is necessary for otoconial seeding and nucleation [9-11]. Oc90 can bind
40 Otolin-1 to establish a protein-rich matrix that serves as a scaffold for subsequent deposition of
41 calcium carbonate [12, 13]. While it is not the major protein component in zebrafish otoliths, Oc90
42 plays an important role in otolith seeding and early development as *oc90*-morphants do not develop

43 otoliths [1, 14, 15]. While additional gene mutations have been identified that lead to otolith agenesis
44 [16-20], the genes responsible for several zebrafish otolith mutants have been undetermined.

45 In this study, we sought to identify and characterize the causative gene in a pair of genetically-
46 linked mutants, *no content* (*nco*) and *corkscrew* (*csr*), that fail to develop otoliths during early inner ear
47 development. We provide genetic evidence that the causative gene is polyketide synthase (*pks1*;
48 currently *wu:fc01d11*), a candidate gene that was recently identified as a key factor of otolith
49 biomineralization in Japanese medaka (*Oryzias latipes*) [21].

50 2. Materials and Methods

51 All zebrafish were maintained in a temperature-controlled (28.5°C) and light-controlled (14h
52 on/10h off) room per standardized conditions. *nco* strain (jj149) was generated by an ENU screen and
53 obtained from ZIRC (Eugene, OR, USA). *csr* was a spontaneous mutant in a *bre*-KO2/*ntl*-GFP line. All
54 protocols (0924) were approved by Creighton University IACUC.

55 Mutant *nco* embryos and wild-type (WT) clutchmates were collected during the critical period
56 of otolith nucleation and seeding (24 hours post fertilization, hpf) and submitted for RNA sequencing.
57 Analysis was completed using MMAPPR (Mutation Mapping Analysis Pipeline for Pooled RNA-seq)
58 [22]. Whole genome sequencing of *csr* was performed and analyzed using MegaMapper [23]. All
59 sequencing was conducted at the University of Nebraska Medical Center Genomics Core Facility.
60 Accession numbers for *nco* RNA-seq and *csr* genome sequencing will be provided during review.

61 WT mRNA and *pks1*^{L905P} was synthesized using mMessage Machine from a clone provided by
62 Dr. Hiroyuki Takeda (University of Tokyo), cleaned on an RNeasy column, and subsequently
63 injected into single-cell *csr* and *nco* embryos. Site-directed mutagenesis was used to generate the
64 mutant clone containing the causative mutation in *csr* (*pks1*^{L905P} in Japanese medaka; *pks1*^{A911P} in
65 zebrafish). Primers used for site-directed mutagenesis were:

66 *pks1*_{L905P}_Forward: 5'-GATATGGCGTGATGTCCGGTGACAGGTTGAAGATC-3'

67 *pks1*_{L905P}_Reverse: 5'-ATCTCAACCTGTCACCGGACATCACGCCATATC-3'

68 Pathway analysis of *nco* was performed using Ingenuity Pathway Analysis (IPA,
69 <http://www.ingenuity.com>) [24]. The Ensembl Gene IDs for differentially expressed genes were
70 uploaded to IPA. Cut-off for gene expression analysis was set at 0.75 RPKM. The calculated z-score
71 indicates a pathway with genes exhibiting increased mRNA levels (positive) or decreased mRNA
72 levels (negative). No change in mRNA levels results in a z-score of zero.

73 *csr* and *nco* were PCR-amplified and submitted for Sanger sequencing using the following
74 primers:

75 *nco*_Forward: 5'-GGGAGGATGCTTGTGTTGG-3'

76 *nco*_Reverse: 5'-GTGGCCCAGAATAGGATCCA-3'

77 *csr*_Forward: 5'-AAGACGGGGACATGACTCAG-3'

78 *csr*_Reverse: 5'-TTCAACAAACAGTGCTCCGG-3'

79 *csr* and *nco* embryos were collected during key stages in ear development, fixed with hydrogel
80 and washed in CHAPS-based CLARITY-clearing solution [25]. Embryos were decalcified with EDTA
81 before blocking, incubating in primary and secondary antibodies diluted in PBS-Triton (0.1%), and
82 imaging by confocal microscopy. Affinity-purified rabbit polyclonal antibodies were generated to
83 Otogelin (1:1000), Otoconin-90 (1:1000), or Starmaker (1:1000) peptides by conventional methods and
84 directly labelled before immunofluorescence. Other antibodies used were Keratan Sulfate (MZ15;
85 1:2000; DSHB), Hair Cell Specific-1 (HCS-1; 1:500; DSHB), and acetylated-tubulin (1:500; Sigma
86 T6793). Phalloidin (ThermoFisher A12379) was used at a concentration of 1:500.

87 Mitotracker Red (ThermoFisher #M22425) was resuspended in DMSO (0.25 mM) and diluted to
88 200 nM in E3 embryo medium. Embryos were then incubated for 20 minutes before removing
89 Mitotracker solution and replacing with fresh E3 embryo medium. Samples were allowed to stabilize
90 for 30 minutes before imaging at 21 hpf. Embryos were phenotyped at 27 hpf.

91 To test the effects of exogenous calcium ions on otolith formation, embryos were kept in E3
92 Medium until early gastrulation. Embryos were washed, dechorionated, and transferred to 1X Basic
93 Solution (58 mM NaCl, 0.4 mM MgSO₄ and 5 mM HEPES) supplemented with 0.7 mM potassium
94 chloride [0 mM Ca²⁺], 0.6 mM calcium nitrate [0.15 mM Ca²⁺] or 0.6 mM calcium chloride [0.22 mM
95 Ca²⁺]. Embryos were then transferred to fresh 1X Basic Solution with respective supplement for the
96 remaining development. Embryos were scored by the presence or absence of otoliths at 27 hpf.

97 Statistical significance was calculated using Fisher's Exact Test and Chi-Squared Distribution or
98 by Linear Regression.

99 3. Results

100 3.1 *csr* and *nco* are genetically-linked

101 The most apparent phenotype of *csr* and *nco* mutants is that they fail to form otoliths or any
102 observable complex calcium deposits within the inner ear (Fig. 1A-C). Furthermore, the mutant
103 larvae are homozygous lethal as the swim bladder fails to inflate (Fig. 1A'-C') and they are unable to
104 feed. While it is still unknown why the swim bladder fails to inflate when otoliths are absent, it is a
105 common phenotype in other mutants with otolith agenesis [14, 16-18, 22]. Due to this commonality
106 within *csr* and *nco* content, we sought to determine if these phenotypes would complement each
107 other. The results of the complementation test showed that mutants failed to develop otoliths (n =
108 31/106), supporting that *nco* and *csr* likely are allelic.

109 3.2 Exogenous calcium ions influence otolith nucleation in *csr* embryos; not *nco* embryos

110 As an aquatic species, the environment of zebrafish can be easily controlled and adapted to
111 assess its impact on embryonic development. Previously, small molecules have been used to block
112 otolith development by inhibiting otolith nucleation [6]. While the endolymph is low in calcium ions
113 [2], we hypothesized that there was an error in calcium ion homeostasis that could be affected by
114 exogenous solutions. We treated both *csr* and *nco* embryos with varying calcium ion concentrations.
115 In water treatments supplemented with potassium chloride ([0 mM Ca²⁺]; n = 59), we found a
116 significant increase in *csr* embryos lacking otoliths (p = 0.029) (Fig. S1). In *csr* embryos treated with
117 calcium chloride ([0.22 mM Ca²⁺]; n = 64), we observed a partial rescue of normal otolith formation;
118 however, it was not statistically significant (p = 0.148). Furthermore, we observed no significant
119 change in the frequency of mutant phenotype in calcium nitrate-treated embryos ([0.15 mM Ca²⁺]; n
120 = 119). Additionally, we observed no significant change in *nco* embryos for water treatments
121 supplemented with potassium chloride ([0 mM Ca²⁺]; n = 107) or calcium chloride ([0.22 mM Ca²⁺]; n
122 = 120) compared to calcium nitrate-treated embryos ([0.15 mM Ca²⁺]; n = 112). Overall, exogenous
123 calcium concentrations correlate with penetrance of otolith formation in *csr* embryos (R² = 0.9978);
124 however, *nco* embryos were unaffected (R² = 0.7802). Furthermore, Mitotracker was used to mark
125 mitochondria-rich cells in *csr* and *nco* embryos. While *nco* embryos appear normal, we observed that
126 *csr* embryos show a lack of Mitotracker localization at 21 hpf (Fig. S2). Altogether, this suggests the
127 nature of each mutation, while likely allelic, are inherently different.

128 3.3 Potentially deleterious mutations identified in polyketide synthase for *csr* and *nco*

129 To positionally clone the gene responsible for *nco* and *csr*, we used complementary approaches
130 for each strain. MMAPPR analysis of *nco*-derived RNA sequencing (Fig. 2A) [22] and MegaMapper
131 analysis of *csr*-derived whole genome sequencing (Fig. 2B) [23] both identified a genomic region with
132 high homology surrounding the *pks1* locus. While several other genes were in that region, a previous
133 study on otolith biomineralization in Japanese medaka made *pks1* the likely gene candidate [21].
134 Potentially deleterious mutations were identified in *pks1* for *csr* (A911P) and *nco* (L681*), which were
135 both located within a conserved acyl transferase domain (Fig. 2C).

136 3.4 Japanese medaka *pks1* mRNA rescues otolith biomineralization in *csr* and *nco*

137 While the last common ancestor of Japanese medaka and zebrafish was estimated to be 150
138 million years ago [26], we sought to assess if the function of *pks1* within the inner ear is conserved.
139 We injected Japanese medaka *pks1* mRNA into single-cell embryos of *csr* and *nco* incrosses at a
140 concentration of 300 ng/ μ L. Microinjection of Japanese medaka *pks1* mRNA rescued otolith
141 biomineralization in both *csr* ($p < 0.0001$; $\chi^2 < 0.0001$; $n = 93$) and *nco* ($p = 0.0032$; $\chi^2 = 0.0022$; $n = 84$) mutants
142 (Fig. 3B). Using site-directed mutagenesis, we introduced the non-synonymous mutation (A911P) in
143 *csr* to the Japanese medaka mRNA construct (L905P). We repeated injections into single-cell embryos
144 and failed to rescue otolith biomineralization in *csr* and *nco*. WT medaka *pks1*, but not *pks1*^{L905P},
145 rescued otolith biomineralization in *csr* and *nco* embryos (Fig. 3C).

146 3.5 Ingenuity pathway analysis of *nco* embryos

147 While *pks1* is thought to produce an otolith nucleation factor [21], its broader role during inner
148 ear development is unknown. Ingenuity Pathway Analysis of *nco* at 24 hpf identified eNOS signaling
149 and Endothelin-1 signaling as the top up- and down-regulated pathways, respectively (Fig. 4A).
150 Among the down regulated genes was *rdh12l*, a gene adjacent to *pks1*, suggesting that there is local
151 control of transcription at that loci. *mir-92a*, the top down-regulated gene, has a predicted binding
152 site in the 3'UTR of *rdh12l* (Fig. S3) [27]. In addition, several genes listed in the top ten up- or down-
153 regulated lists are also enriched in adult mechanosensory hair cells such as *il11b*, *fosab*, *fosb*, *fosl1a*,
154 *socs3a*, *scg5*, and *dnaaf3* (Figs. 4B-C) [28]. Of these genes, *il11b* is up-regulated during neuromast hair
155 cell regeneration [29]. Notably, *dnaaf3* causes primary ciliary dyskinesia and morpholino knockdown
156 of *dnaaf3* causes abnormal otolith growth [30]. While its role in inner ear development is unknown,
157 *scg5* is expressed within the anterior and posterior poles of the otic placode during the critical period
158 of otolith nucleation [31].

159 3.6 Aberrant expression of proteins involved in otolith development in *csr* and *nco*

160 In mammalian inner ear development, Oc90 is necessary for otoconial seeding and nucleation
161 [9, 10]. Similarly, the role of Oc90 is evolutionally conserved in zebrafish and has been previously
162 thought to be sufficient for otolith nucleation [14]. Using immunofluorescence (IF), we saw diffuse
163 expression of Oc90 in *csr* and *nco* otocysts (Figs. 5B-D), which demonstrated that Oc90 expression
164 within the otocyst is not sufficient for otolith biomineralization in zebrafish. Similarly, normal
165 localization of Otogelin (Otog), a protein required for otolith tethering in the otolithic membrane is
166 not sufficient for Oc90 attachment. Additionally, other otoconins that are important for calcium

167 deposition and growth were detected with diffuse expression within the otocyst such as Starmaker
168 and Keratan Sulfate (data not shown) [32, 33].

169 3.7 Polyketide synthase expression enriched in adult mechanosensory hair cells

170 Otolith nucleation is thought to be mediated by a tether-cell specific otolith precursor binding
171 factor (OPBF), which lays the foundation for the successive biomineralization of the otolith [5, 7, 34].
172 The presence of an OPBF was proposed almost two decades ago and its identification proves to be
173 elusive [34]. Recent studies suggest that one or more OPBFs are expressed by tether-cells and help to
174 mediate otolith nucleation by binding other OPPs [5, 7, 35].

175 We sought to assess if *pks1* or its enzymatic product is a tether-cell OPBF. First, we demonstrate
176 that the total number of hair cells remain unchanged during early development in *nco*, suggesting
177 there are no differences in tether cell maturation and maintenance (Figs. 5E-G). Then, using publicly
178 available RNA-seq data, *pks1* mRNA can be detected during the critical period of otolith nucleation
179 [36]. Previous data has shown its localization in the otic vesicle at 19 hpf [21], supporting its role as
180 an OPBF. *pks1* is enriched (7.46-fold increase) in mechanosensory hair cells compared to support cells
181 within the adult zebrafish inner ear (Table S1). Additionally, RNA-seq data suggests *pks1* appears to
182 be differentially expressed in support cells. Support cells predominantly express a 300bp region of
183 the 5'UTR of the *pks1* transcript [28]. A search for transcriptional regulatory motifs in the 5'UTR of
184 *pks1* found a predicted binding site for TCF-3, a transcription factor highly expressed in adult
185 mechanosensory hair cells [28], has a potential binding site there [37]. While the role of TCF-3 in the
186 inner ear is unknown, it is expressed within the otic vesicle during the critical period of otolith
187 nucleation [31].

188 4. Discussion

189 The mutants *csr* and *nco* were chosen for this study because each lack the necessary factors
190 such as an OPBF for otolith seeding and biomineralization. To determine the genes responsible for
191 otolith agenesis in these mutants, we used two complementary approaches. The first approach was
192 Whole Genome Sequencing of the *csr* mutant genome to identify regions of high homology. This
193 indeed was difficult as the *csr* background strain was heavily inbred, resulting in multiple peaks of
194 high homology. Since we demonstrated *csr* and *nco* are genetically-linked, we sought to further
195 clarify the responsible locus using a second method (i.e. RNA-seq of the *nco* transcriptome) for
196 comparison. This result pinpointed a region of high homology near the end of the 24th chromosome.
197 While deciphering potentially deleterious mutations within that region, we focused on *pks1*
198 following evidence that it is responsible for otolith nucleation in Japanese medaka [21]. While these
199 species are evolutionarily divergent, the shared phenotype between medaka and our mutants
200 suggested that the role of *pks1* is conserved. As a result, we chose to use medaka *pks1* mRNA to
201 rescue otolith formation in *csr* and *nco*. Similarities can also be drawn with other zebrafish mutants
202 such as *keinstein* which has diffuse expression of Starmaker within the otocyst and exhibits similar
203 circling swimming behaviors [38, 39]. Furthermore, *keinstein* may be another *pks1* allele due to its
204 predicted chromosomal location [40].

205 While WT medaka *pks1* rescues otolith biomineralization in *csr* and *nco*, differences in penetrance
206 of calcium ions on otolith formation suggested the nature of each mutation is fundamentally
207 different. This was confirmed by Sanger sequencing that *nco* has a premature stop codon while *csr*
208 likely makes a defective protein that may be stabilized by exogenous calcium. This defective protein

209 may be the explanation for the differences in Mitotracker localization in *csr*. Due to its surface stain
210 expression, we hypothesize that Mitotracker was localized to mitochondria-rich ionocytes [41].
211 Ionocytes have previously been implicated in otolith formation as mutations in *gcm2*, which is
212 responsible for ionocyte maturation, leads to otolith agenesis [42]. We hypothesize that the
213 endolymph in *csr* and *nco* mutants has the necessary components for otolith nucleation [2] but lack a
214 trigger produced by *pks1*. Additionally, the absence of *pks1* does not visibly appear to affect hair cell
215 development that are required for otolith nucleation [5]. IF of *csr* and *nco* embryos demonstrated that
216 expression of a critical otoconial seeding protein, Oc90, within the otocyst is not sufficient for otolith
217 biomineralization in the presence of the otolith membrane.

218 While *pks1* likely acts as an enzyme whose expression is enriched in adult mechanosensory hair
219 cells [28], its product acts as an OPBF and is required for otolith nucleation in zebrafish. However,
220 the molecular function of *pks1* remains unknown. Using *nco* RNA-seq data, we could perform an
221 Ingenuity Pathway Analysis, which identified eNOS signaling and Endothelin-1 signaling as the
222 most up- and down-regulated pathways, respectively. eNOS signaling could be impacted by *pks1*
223 metabolites such as iromycin, which has been shown to inhibit eNOS signaling [43]. Both eNOS and
224 Endothelin-1 have been implicated in inner ear development and function. Notably, it has been
225 demonstrated that these pathways are inversely related in sensorineural hearing loss [44]. An
226 example of this is Waardenburg syndrome, caused by mutations in endothelins, which cause
227 abnormal pigmentation and sensorineural hearing loss [45]. During early development, Endothelin-
228 1 mRNA turns on during the critical period of otolith nucleation [31, 36] and is detected in the otic
229 vesicle at 24 hpf [46]. Endothelin-1 and its receptor (*ednraa*) are both enriched in adult zebrafish inner
230 ear support cells [28]. Additionally, Endothelin-1 has been implicated with the FOS-family of genes
231 (*fosab*, *fosb*, and *fosl1a*) and *socs3a*, which are all differentially expressed in *nco* at 24 hpf. They are all
232 part of a regulatory network during hypergravity-mediated bone formation [47], which might
233 suggest a common mechanism between bone mineralization and otolith biomineralization. Future
234 studies will attempt to clarify the roles of Endothelin-1 and eNOS signaling pathways during otolith
235 biomineralization.

236 **Author Contributions:** Conceptualization, K.T. and K.K.; Methodology, K.T. and K.K.; Validation, K.T. and
237 L.H.; Formal Analysis, K.T.; Investigation, K.T. and L.H.; Resources, K.K.; Data Curation, K.K.; Writing-
238 Original Draft Preparation, K.T.; Writing-Review & Editing, K.T. and K.K.; Visualization, K.T. and K.K.;
239 Supervision, K.K.; Project Administration, K.K.; Funding Acquisition, K.K.

240 **Funding:** We are grateful for funding through grants from the State of Nebraska (LB-692), the National Center
241 for Research Resources (5P20RR018788-09), and the National Institute of General Medical Sciences (8 P20
242 GM103471-09).

243 **Acknowledgments:** We thank the University of Nebraska Medical Center Genomics Core Facility for
244 assistance with sequencing and bioinformatics. We thank Dr. Hiroyuki Takeda from the University of Tokyo
245 for supplying the Japanese medaka *pks1* mRNA construct. We thank Creighton University Integrated
246 Biomedical Imaging Facility for assistance with confocal microscopy. We thank the members of the Kramer
247 Lab at Creighton University for their support with zebrafish husbandry.

248 **Conflicts of Interest:** The authors declare no conflict of interest.

249

250 **References**

- 251 1. Lundberg, Y.W., et al., *Mechanisms of otoconia and otolith development*. Dev Dyn, 2015. **244**(3): p.
252 239-53.
- 253 2. Payan, P., et al., *Endolymph chemistry and otolith growth in fish*. Comptes Rendus Palevol, 2004.
254 **3**(6-7): p. 535-547.
- 255 3. Borelli, G., et al., *Biochemical relationships between endolymph and otolith matrix in the trout*
256 *(Oncorhynchus mykiss) and turbot (Psetta maxima)*. Calcif Tissue Int, 2001. **69**(6): p. 356-64.
- 257 4. Riley, B.B., et al., *A critical period of ear development controlled by distinct populations of ciliated*
258 *cells in the zebrafish*. Dev Biol, 1997. **191**(2): p. 191-201.
- 259 5. Stooke-Vaughan, G.A., et al., *The role of hair cells, cilia and ciliary motility in otolith formation in*
260 *the zebrafish otic vesicle*. Development, 2012. **139**(10): p. 1777-87.
- 261 6. Peterson, R.T., et al., *Small molecule developmental screens reveal the logic and timing of vertebrate*
262 *development*. Proc Natl Acad Sci U S A, 2000. **97**(24): p. 12965-9.
- 263 7. Stooke-Vaughan, G.A., et al., *Otolith tethering in the zebrafish otic vesicle requires Otogelin and*
264 *alpha-Tectorin*. Development, 2015. **142**(6): p. 1137-45.
- 265 8. Riley, B.B., *Genes Controlling the Development of the Zebrafish Inner Ear and Hair Cells*, in
266 *Current Topics in Developmental Biology*. 2003, Academic Press. p. 357-388.
- 267 9. Zhao, X., et al., *Otoconin-90 deletion leads to imbalance but normal hearing: a comparison with*
268 *other otoconia mutants*. Neuroscience, 2008. **153**(1): p. 289-99.
- 269 10. Zhao, X., et al., *Gene targeting reveals the role of Oc90 as the essential organizer of the otoconial*
270 *organic matrix*. Dev Biol, 2007. **304**(2): p. 508-24.
- 271 11. Wang, Y., et al., *Otoconin-90, the mammalian otoconial matrix protein, contains two domains of*
272 *homology to secretory phospholipase A2*. Proc Natl Acad Sci U S A, 1998. **95**(26): p. 15345-50.
- 273 12. Deans, M.R., J.M. Peterson, and G.W. Wong, *Mammalian Otolin: a multimeric glycoprotein specific*
274 *to the inner ear that interacts with otoconial matrix protein Otoconin-90 and Cerebellin-1*. PLoS
275 One, 2010. **5**(9): p. e12765.
- 276 13. Moreland, K.T., et al., *In vitro calcite crystal morphology is modulated by otoconial proteins otolin-*
277 *1 and otoconin-90*. PLoS One, 2014. **9**(4): p. e95333.
- 278 14. Petko, J.A., et al., *Otoc1: a novel otoconin-90 ortholog required for otolith mineralization in*
279 *zebrafish*. Dev Neurobiol, 2008. **68**(2): p. 209-22.
- 280 15. Murayama, E., et al., *Otolith matrix proteins OMP-1 and Otolin-1 are necessary for normal otolith*
281 *growth and their correct anchoring onto the sensory maculae*. Mech Dev, 2005. **122**(6): p. 791-803.
- 282 16. Hughes, I., et al., *Otopetrin 1 is required for otolith formation in the zebrafish Danio rerio*. Dev Biol,
283 2004. **276**(2): p. 391-402.
- 284 17. Stawicki, T.M., et al., *The zebrafish merovingian mutant reveals a role for pH regulation in hair cell*
285 *toxicity and function*. Dis Model Mech, 2014. **7**(7): p. 847-56.
- 286 18. Sumanas, S., J.D. Larson, and M. Miller Bever, *Zebrafish chaperone protein GP96 is required for*
287 *otolith formation during ear development*. Dev Biol, 2003. **261**(2): p. 443-55.
- 288 19. Kiss, P.J., et al., *Inactivation of NADPH oxidase organizer 1 results in severe imbalance*. Curr Biol,
289 2006. **16**(2): p. 208-13.
- 290 20. Colantonio, J.R., et al., *The dynein regulatory complex is required for ciliary motility and otolith*
291 *biogenesis in the inner ear*. Nature, 2008. **457**: p. 205.

- 292 21. Hojo, M., et al., *Unexpected link between polyketide synthase and calcium carbonate*
293 *biomineralization*. *Zoological Lett*, 2015. **1**(1): p. 3.
- 294 22. Hill, J.T., et al., *MMAPPR: Mutation Mapping Analysis Pipeline for Pooled RNA-seq*. *Genome*
295 *Research*, 2013. **23**(4): p. 687-697.
- 296 23. Obholzer, N., et al., *Rapid positional cloning of zebrafish mutations by linkage and homozygosity*
297 *mapping using whole-genome sequencing*. *Development*, 2012. **139**(22): p. 4280-90.
- 298 24. Kramer, A., et al., *Causal analysis approaches in Ingenuity Pathway Analysis*. *Bioinformatics*, 2014.
299 **30**(4): p. 523-30.
- 300 25. Chung, K., et al., *Structural and molecular interrogation of intact biological systems*. *Nature*, 2013.
301 **497**(7449): p. 332-7.
- 302 26. Kirchmaier, S., et al., *The Genomic and Genetic Toolbox of the Teleost Medaka (*Oryzias latipes*)*.
303 *Genetics*, 2015. **199**(4): p. 905-918.
- 304 27. Ulitsky, I., et al., *Extensive alternative polyadenylation during zebrafish development*. *Genome Res*,
305 2012. **22**(10): p. 2054-66.
- 306 28. Barta, C.L., et al., *RNA-seq transcriptomic analysis of adult zebrafish inner ear hair cells*. *Sci Data*,
307 2018. **5**: p. 180005.
- 308 29. Jiang, L., et al., *Gene-expression analysis of hair cell regeneration in the zebrafish lateral line*.
309 *Proceedings of the National Academy of Sciences*, 2014. **111**(14): p. E1383-E1392.
- 310 30. Mitchison, H.M., et al., *Mutations in axonemal dynein assembly factor DNAAF3 cause primary*
311 *ciliary dyskinesia*. *Nature Genetics*, 2012. **44**: p. 381.
- 312 31. Thisse, B., et al., *Expression of the zebrafish genome during embryogenesis*. 2001: ZFIN Direct Data
313 Submission.
- 314 32. Yang, H., et al., *Matrix recruitment and calcium sequestration for spatial specific otoconia*
315 *development*. *PLoS One*, 2011. **6**(5): p. e20498.
- 316 33. Sollner, C., et al., *Control of crystal size and lattice formation by starmaker in otolith*
317 *biomineralization*. *Science*, 2003. **302**(5643): p. 282-6.
- 318 34. Riley, B.B. and D.J. Grunwald, *A mutation in zebrafish affecting a localized cellular function*
319 *required for normal ear development*. *Dev Biol*, 1996. **179**(2): p. 427-35.
- 320 35. Yu, X., et al., *Cilia-driven fluid flow as an epigenetic cue for otolith biomineralization on sensory*
321 *hair cells of the inner ear*. *Development*, 2011. **138**(3): p. 487-94.
- 322 36. White, R.J., et al., *A high-resolution mRNA expression time course of embryonic development in*
323 *zebrafish*. *Elife*, 2017. **6**.
- 324 37. Chang, T.H., et al., *An enhanced computational platform for investigating the roles of regulatory*
325 *RNA and for identifying functional RNA motifs*. *BMC Bioinformatics*, 2013. **14 Suppl 2**: p. S4.
- 326 38. Sollner, C., et al., *Mutated otopetrin 1 affects the genesis of otoliths and the localization of*
327 *Starmaker in zebrafish*. *Dev Genes Evol*, 2004. **214**(12): p. 582-90.
- 328 39. Whitfield, T.T., et al., *Mutations affecting development of the zebrafish inner ear and lateral line*.
329 *Development*, 1996. **123**: p. 241-54.
- 330 40. Geisler, R., et al., *Large-scale mapping of mutations affecting zebrafish development*. *BMC*
331 *Genomics*, 2007. **8**: p. 11.
- 332 41. Esaki, M., et al., *Mechanism of development of ionocytes rich in vacuolar-type H(+)-ATPase in the*
333 *skin of zebrafish larvae*. *Developmental biology*, 2009. **329**(1): p. 116-129.

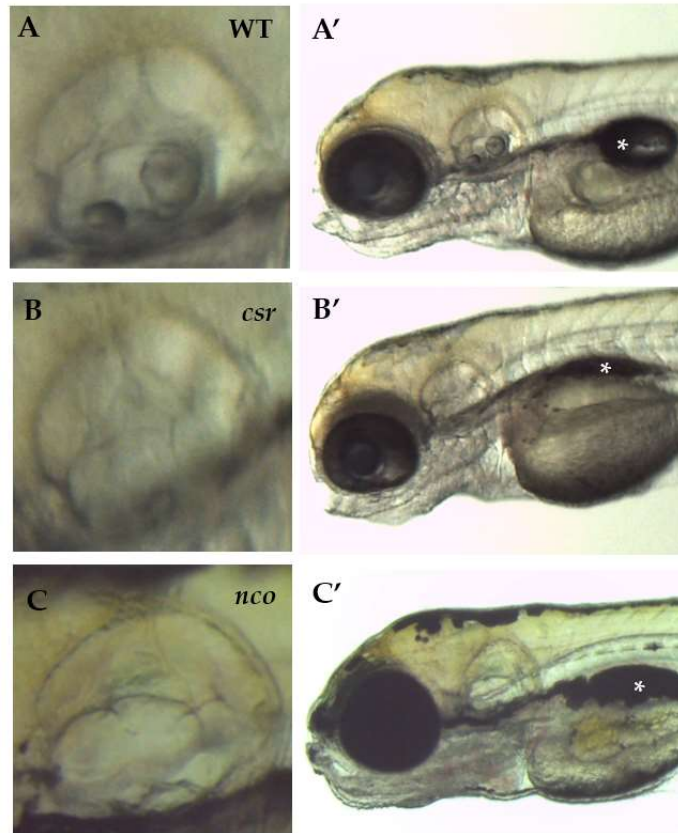
- 334 42. Kumai, Y., R.W.M. Kwong, and S.F. Perry, *A role for transcription factor glial cell missing 2 in*
335 *Ca²⁺ homeostasis in zebrafish, Danio rerio*. Pflügers Archiv - European Journal of Physiology,
336 2015. **467**(4): p. 753-765.
- 337 43. Surup, F., et al., *The iromycins, a new family of pyridone metabolites from Streptomyces sp. I.*
338 *Structure, NOS inhibitory activity, and biosynthesis*. J Org Chem, 2007. **72**(14): p. 5085-90.
- 339 44. Liu, Q., et al., *[The study on plasma ET and NO of patients with sudden hearing loss]*. Lin Chuang
340 Er Bi Yan Hou Ke Za Zhi, 2003. **17**(11): p. 668-9.
- 341 45. Pingault, V., et al., *Review and update of mutations causing Waardenburg syndrome*. Hum Mutat,
342 2010. **31**(4): p. 391-406.
- 343 46. Miller, C.T., et al., *sucker encodes a zebrafish Endothelin-1 required for ventral pharyngeal arch*
344 *development*. Development, 2000. **127**(17): p. 3815-3828.
- 345 47. Aceto, J., et al., *Zebrafish Bone and General Physiology Are Differently Affected by Hormones or*
346 *Changes in Gravity*. PLoS ONE, 2015. **10**(6): p. e0126928.



© 2018 by the authors. Submitted for possible open access publication under the terms and conditions of the Creative Commons Attribution (CC BY) license

349 (<http://creativecommons.org/licenses/by/4.0/>).

350



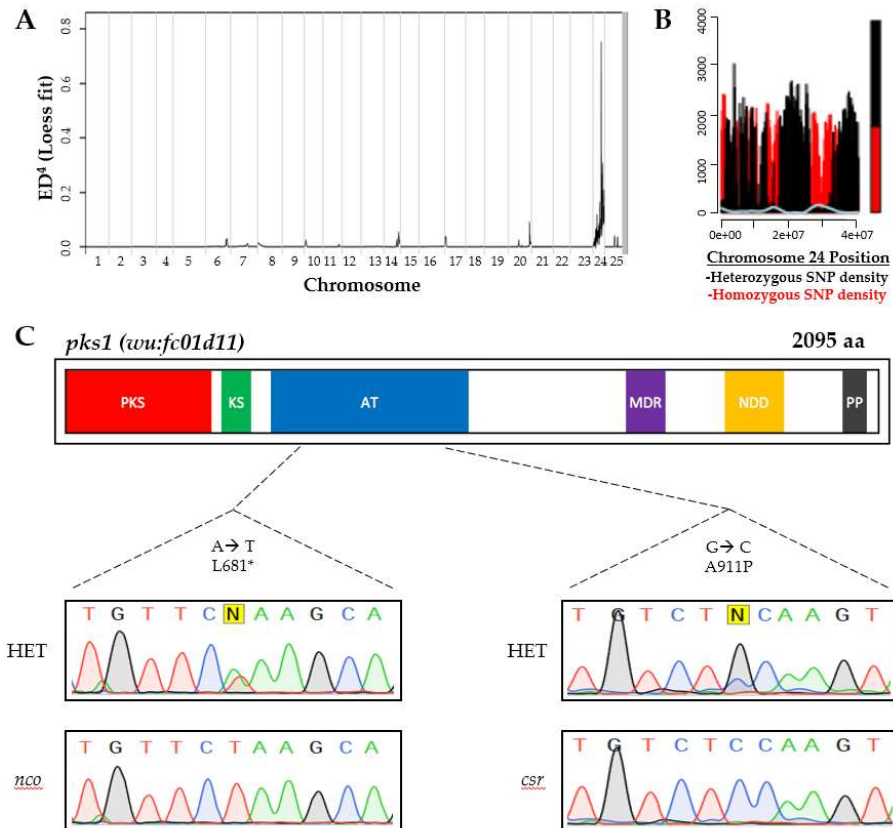
351

352

353

354

Figure 1: (A-C) The *csr* and *nco* mutant phenotypes fail to form otoliths within the inner ear. However, semicircular canal formation appears to be normal. (A'-C') Both mutants fail to inflate their swim bladders, which is lethal. Imaged at 5 days post fertilization (dpf). Magnification 6.3X. (*) indicates swim bladder.



355

356

357

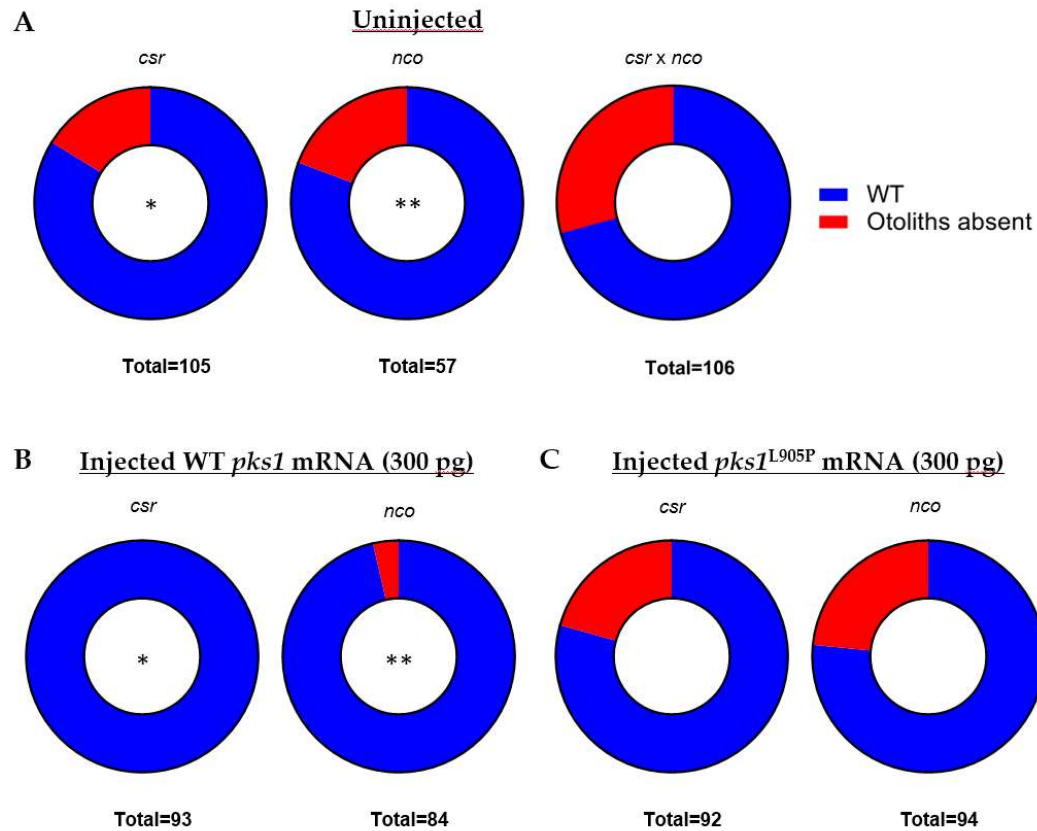
358

359

360

361

Figure 2: Complementary approaches for causative gene discovery. MMAPPR analysis of RNA sequencing data for *nco* (A) and whole genome homology mapping for *csr* (B) identified regions of high homology on the 24th chromosome near the *pks1* locus (~33 Gb). (C) Causative mutations were identified in *pks1* for *nco* and *csr* within the acyl transferase (AT) domain. Sanger sequencing confirmed SNPs in *csr* and *nco* mutants. Other domains include Polyketide Synthase (PKS), Ketoacyl Synthetase (KS), Medium Chain Reductase (MDR), NAD(P)-dependent dehydrogenase (NDD), and Phosphopanthetheine-Binding (PP).



362

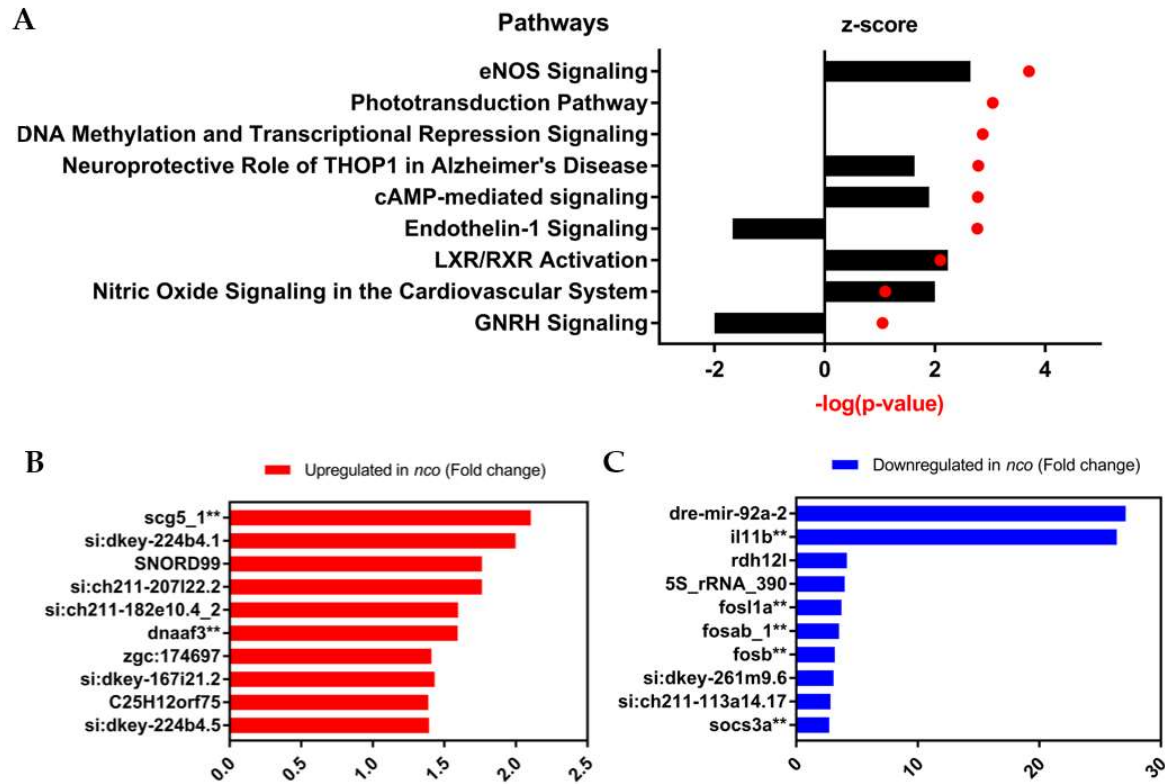
363

364

365

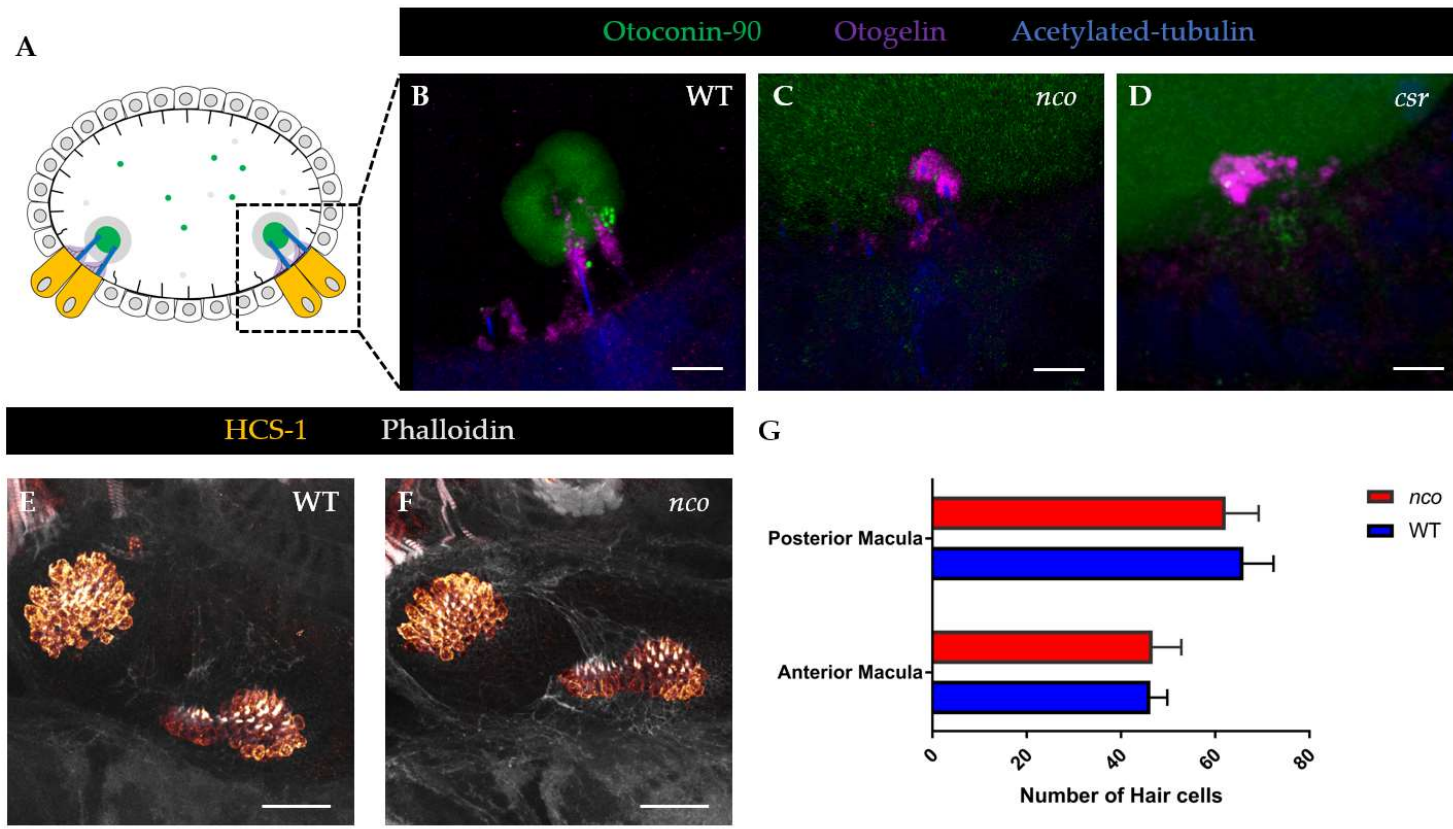
366

Figure 3: WT *pks1* mRNA, not *pks1*^{L905P}, rescues otolith formation in *csr* and *nco*. (A) Normal frequencies of mutant phenotypes in each uninjected strain. All three pairings follow homozygous recessive mode of inheritance. (B) Results of injected embryos show that Japanese medaka *pks1* mRNA (300 pg) rescues both *csr* and *nco* mutants. (*, $p < 0.0001$, paired *t*-test)(**, $p < 0.0032$, paired *t*-test) Site-directed mutagenesis was used to introduce a conserved mutation in *csr* (A911P) into the Japanese medaka construct (L905P) (C) Injection of *pks1*^{L905P} (300 pg) fails to rescue *csr* or *nco* phenotypes.



367
368
369
370
371
372

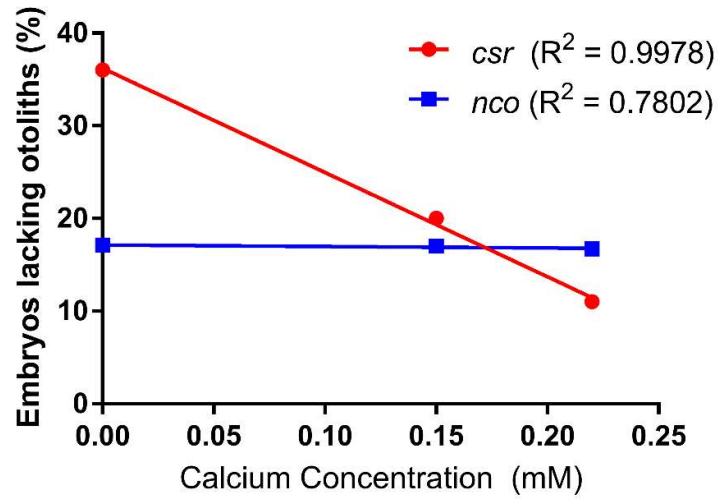
Figure 4: Gene expression and pathway analysis of *nco* embryos. (A) Ingenuity Pathway Analysis shows the top up-regulated and down-regulated pathways, which are eNOS Signaling and Endothelin-1 Signaling, respectively. Positive z-score indicated increased mRNA levels. Negative z-score indicates decreased mRNA levels. No change in mRNA levels results in a z-score of zero. (B) Differential gene expression in the top up-regulated genes. (C) Differential gene expression in the top down-regulated genes. (**, expressed in adult zebrafish mechanosensory hair cells) [28].



373
374
375
376
377

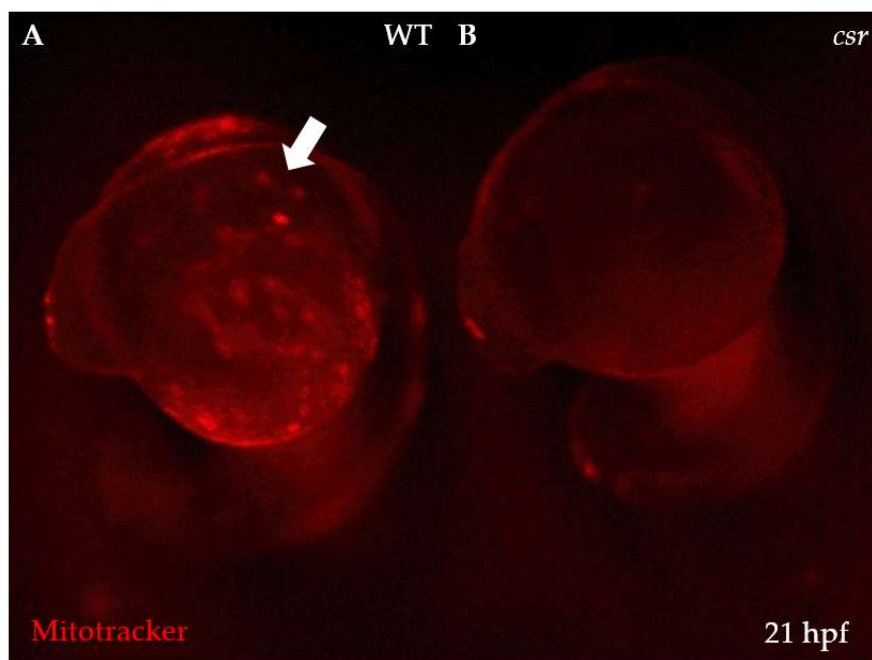
Figure 5: Aberrant expression of proteins involved in otolith development in *csr* and *nco*. (A) Schematic of otic vesicle at 27 hpf. Anterior to right. (B) In WT, Oc90 is expressed within the mineralized otolith, which is situated atop the otolithic membrane (Otog), at 27 hpf. Scale bar = 5 μ m. (C-D) Oc90 has diffuse expression within the otocyst of *csr* and *nco*. In *csr* and *nco*, Otog is localized near the apical surface of hair cells. (E-F) Expression showing hair cells in WT and *nco* larvae at 5dpf. Scale bar = 25 μ m. (G) Quantification of hair cell numbers in the posterior and anterior macula of WT and *nco* (n = 4).

378 Appendix A- Supplemental Material



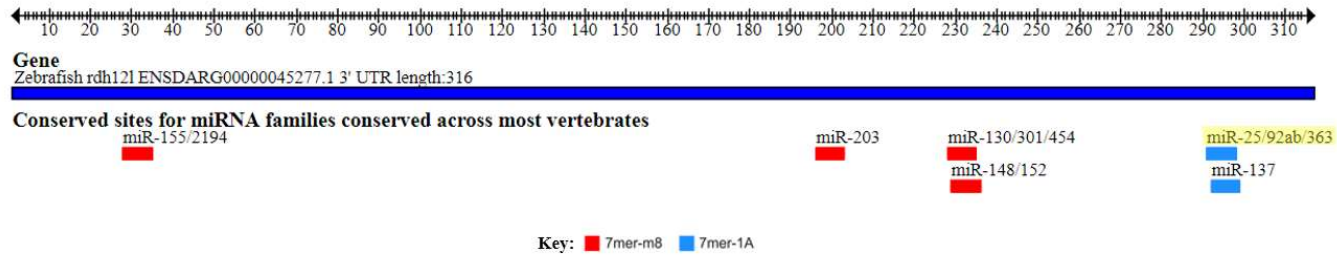
379

380 **Figure S1:** Exogenous calcium ions penetrate otolith nucleation in *csr*. At low calcium concentrations, there is an
381 increase in mutant phenotypes in *csr* compared to standard media. Increasing calcium partially rescued the
382 mutant phenotype. *nco* remained unchanged during all calcium treatments.



383

384 **Figure S2:** Spatial differences in mitochondrial membrane potentials. (A) While Mitotracker marks active
385 mitochondria in WT, (B) *csr* embryos show a lack of Mitotracker expression during early development. Arrow
386 indicates otic vesicle.



387

388 **Figure S3:** *miR-92a* binding site in the 3' UTR of *rdh12l*. TargetScanFish 6.2 of *rdh12l* in zebrafish shows potential microRNA binding sites including *miR-92a*, which is the most
 389 down-regulated gene in *nco* embryos at 24 hpf.

Hair cells (SRA)	Total Reads	ORF - Read Counts	ORF RPKM	5' UTR Read Counts
SRX3022431	14413064	40	0.389182443	0
SRX3022432	100567605	390	0.543821111	0
SRX3022433	50912071	151	0.415916114	0
Support cells (SRA)	Total Reads	ORF - Read Counts	ORF RPKM	5' UTR Read Counts
SRX3022434	54844980	3	0.007670681	14
SRX3022435	59741039	0	0	38
SRX3022436	45498619	0	0	14
			LOG2	
Hair cells RPKM average - ORF		0.44963989	-1.1531	
Hair cells SD		0.082651371		
Support cells RPKM average - ORF		0.002556894	-8.611	
Support cells SD		0.00442867		
Fold Change		7.4579		

390

391 **Table S1.** Differential expression of pks1 in hair and support cells.